

## Update of the trigger system of the PandaX-II experiment

---

**Qinyu Wu,<sup>a</sup> Xun Chen,<sup>a</sup> Xiangdong Ji,<sup>a,b,c,d</sup> Jianglai Liu,<sup>a</sup> Siao Lei,<sup>a</sup> Xiangxiang Ren,<sup>a</sup>  
Meng Wang,<sup>e</sup> Mengjiao Xiao,<sup>a</sup> Pengwei Xie,<sup>a</sup> Binbin Yan,<sup>a</sup> Yong Yang<sup>a</sup>**

<sup>a</sup>*INPAC and Department of Physics and Astronomy, Shanghai Jiao Tong University, Shanghai Laboratory for Particle Physics and Cosmology, Shanghai 200240, China*

<sup>b</sup>*Center of High Energy Physics, Peking University, Beijing 100871, China*

<sup>c</sup>*Department of Physics, University of Maryland, College Park, Maryland 20742, USA*

<sup>d</sup>*T. D. Lee Institute, Shanghai 200240, China*

<sup>e</sup>*School of Physics and Key Laboratory of Particle Physics and Particle Irradiation (MOE), Shandong University, Jinan 250100, China*

*E-mail:* [renxx@sjtu.edu.cn](mailto:renxx@sjtu.edu.cn), [yong.yang@sjtu.edu.cn](mailto:yong.yang@sjtu.edu.cn)

**ABSTRACT:** PandaX-II experiment is a dark matter direct detection experiment using about half-ton of liquid xenon as the sensitive target. The electrical pulses detected by photomultiplier tubes from scintillation photons of xenon are recorded by waveform digitizers. The data acquisition of Pandax-II relies on a trigger system that generates common trigger signals for all waveform digitizers. Previously an analog device-based trigger system was used for the data acquisition system. In this paper we present a new FPGA-based trigger system. The design of this system and trigger algorithms are described. The performance of this system on real data is presented.

**KEYWORDS:** Dark matter experiment, Digital signal processing, Trigger algorithms.

---

## Contents

|          |  |          |
|----------|--|----------|
| <b>1</b> | <b>Introduction of PandaX-II and its data acquisition system</b> | <b>1</b> |
| <b>2</b> | <b>The new PandaX-II trigger system</b>                          | <b>2</b> |
| 2.1      | Overview   | 2        |
| 2.2      | Trigger algorithm  | 3        |
| <b>3</b> | <b>Threshold of the new trigger system</b>                       | <b>5</b> |
| <b>4</b> | <b>Summary</b>   | <b>5</b> |

---

## 1 Introduction of PandaX-II and its data acquisition system

PandaX-II experiment is dark matter (DM) direct detection experiment, located at the China Jin-Ping Underground Laboratory. The primary goal of PandaX-II experiment is to search for weakly interacting massive particle (WIMP)-like DM. PandaX-II operates a dual phase time projection chamber (TPC). The TPC contains 580 kg liquid xenon in the sensitive volume enclosed by polytetrafluoroethylene (PTFE) reflective panels with an inner diameter of 646 mm and a vertical maximum drift length of 600 mm defined by the cathode mesh and gate grid. For each interaction in liquid xenon, both prompt scintillation photons (S1) and delayed electroluminescence photons (S2) are collected by two arrays of 55 Hamamatsu R11410-20 photomultiplier tubes (PMTs) located at the top and bottom, respectively. The time difference between S1 and S2 gives the vertical location of the interaction point in liquid xenon and the charge pattern of S2 signals on the top PMT array gives the horizontal position. The 3-D interaction position can be used to reduce ambient background from detector and surrounding materials. In addition, the ratio of S2 (in unit of Photoelectron, PE) and S1 can be used to discriminate WIMP signals against  $\beta$  and  $\gamma$  backgrounds. More detailed descriptions of the PandaX-II experiment can be found in Ref. [1–3].

The data acquisition (DAQ) system of PandaX-II (see Fig. 1) is very similar as that from the PandaX-I experiment [4]. Signals from PMTs are amplified by a factor of 10 by Phillips 779 amplifiers, and then fed into CAEN V1724 8-channel digitizers [5]. Each channel of the digitizer can produce a time-over-threshold signal and the internal sum of these signals from all channels is output as the so-called Majority (MAJ) signal. MAJ signals from all digitizers and summed by Phillips 740 linear logic Fan In/Out modules. In the old trigger system, which was used in the initial phase of data taking, this MAJ sum signal was integrated by an ORTEC 575A spectroscopy amplifier. The integrated signal was then discriminated by a CAEN V814 VME discriminator to generate the raw trigger signal. The raw trigger signal was fed into CAEN V1495 generic logic that generated the final trigger signal for each V1724 digitizer if not vetoed by the “BUSY” signal from any digitizer. A CAEN V830 scaler counted both the raw and system trigger signals to monitor the system dead-time. More detailed descriptions of the PandaX-I DAQ can be found in Ref. [6].



system is operated under the 50 MHz clock provided by the oscillator on the motherboard. The motherboard output a TTL trigger which is converted to an NIM signal by a gate generator and then converted to an ECL signal by an NIM-ECL convertor. As in the old system, converted raw trigger signals are sent to the generic logic board V1495 for final trigger decision and to the scaler V830 for monitoring.

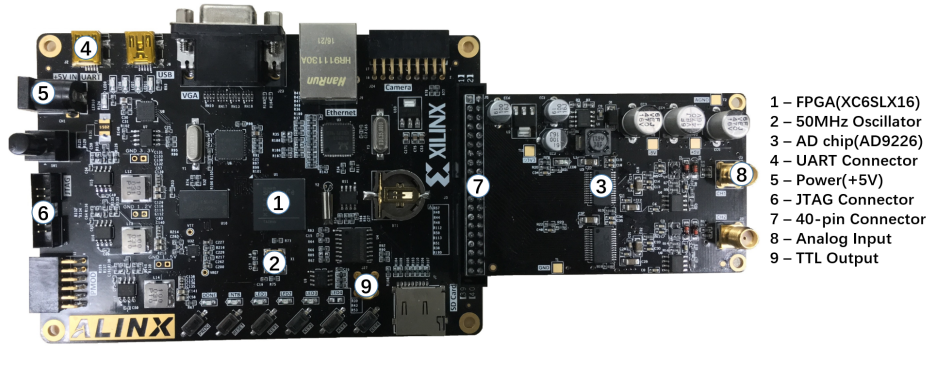


**Figure 2.** A Photo of the FPGA board and the ADC subboard. The ADC board digitizes MAJ sum signal with 12-bit resolution at 50MHz and sends the data to the Xilinx Spartan-6 XC6SLX16 FPGA. The chip processes the data with the loaded algorithm. Parameters in the algorithm can be configured via the UART port.

## 2.2 Trigger algorithm

In this section we describe in detail the algorithm implemented in the FPGA to generate the trigger. The main algorithm calculates the number of peaks, the accumulated time-over-threshold, and the peak amplitude of the incoming digitized data and compare them with preconfigured thresholds. To realize this, we implemented a finite state machine (FSM) in which the present status only depends on the previous status and the present data.

The main algorithm is illustrated in Fig. 3. When the input digitized sample is around the baseline (51 ADC counts in the example), the FSM will stay in the “IDLE” state. When an incoming sample is larger than the threshold (68 in the example), the FSM will change to “PeakUp” state that indicates an incoming peak and this sample is set as the peak amplitude. If the next sample is increasing the FSM will stay in the “PeakUp” state and the peak amplitude will be updated accordingly. If the next sample is decreasing but larger than the threshold, the FSM will change to the “PeakDown” state that indicates the signal is going back to baseline. This peak-finding algorithm will continue until the sample is below the threshold, when the FSM changes to the “Decide” state to check if all conditions on the above-mentioned three variables are satisfied. If not satisfied, the FSM will be in a “Wait” status for a predefined time (peak-wait time, several hundred ns) until another above-threshold sample appears which indicates an incoming peak again. This is because a typical MAJ sum signal from S2 contains a few peaks separated by a few hundred ns.

Once a trigger signal is generated, the FSM will stay in a “TriggerWait” state for a predefined time (trigger-wait time, several ms) to avoid generating multiple triggers for large S2 signals. For very large S2 signals (indicated by very large peak amplitude) it will wait even longer till the

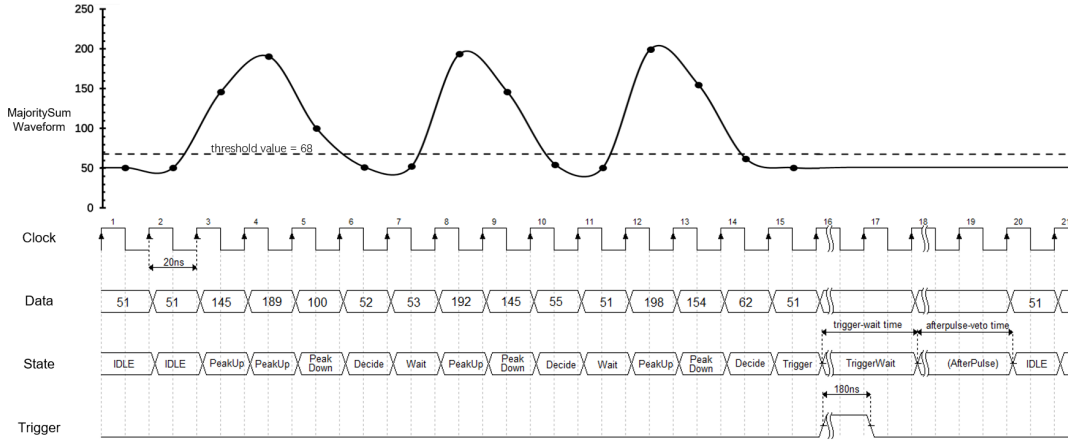


**Figure 3.** An example of the finite state machine loop in the main algorithm.

afterpulse comes back to baseline. After that, the FSM goes back to “IDLE” state and is ready for processing data and generating a new trigger when all conditions satisfied again. An example of a large S2 signal with long afterpulse is shown in Fig. 4 left, where only one trigger signal is generated. We found in the same neutron calibration run condition, though the trigger rate of the new trigger system was 30% higher compared to the old one, the raw data size was reduced by 20% due to less afterpulse data were collected.

Another problem for data acquisition system is the so-called discharge events which could generate multiple triggers and causes system dead time. The data exhibit very low amplitude but prolonged pulse trains. To mitigate this problem, we implemented a discharge-veto module in FPGA to identify discharge signals, which usually have quite long accumulated time-over-threshold. Once a discharge event is identified, a long veto signal will be applied and no trigger signal will be generated. An example of discharge event is shown in Fig. 4 right. We found in this case, the new trigger system generated 8 0% less trigger signals compared to old one.

All the above-mentioned parameters such as peak-wait time, trigger-wait time and thresholds are configurable through the UART port shown in Fig. 2.

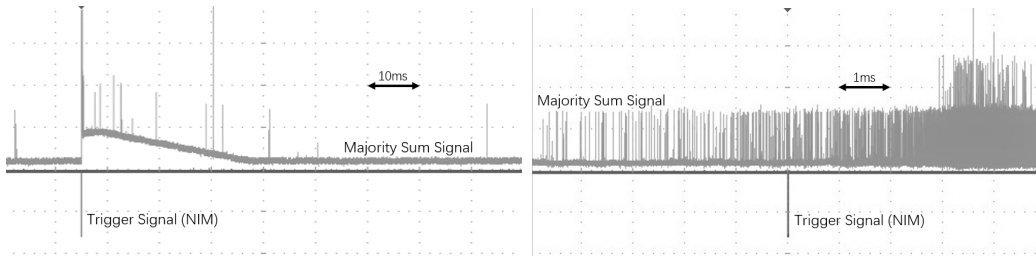


**Figure 4.** a) Left: An oscilloscope screen shot of a long afterpulse following a large S2 signal. The jump of the baseline is due to the Fan-In/Out module that sums up the majority signals. The tail is larger than 30 ms. The FPGA program will wait till the afterpulse comes back to baseline and generate another new trigger when satisfied. b) Right: An oscilloscope screen shot of a discharge event. A veto module is implemented in the FPGA to avoid generating multiple triggers.

### 3 Threshold of the new trigger system

Besides the above-mentioned ability of the new trigger system to mitigate problems due to after-pulses or discharging events, another key performance is the trigger efficiency on S2 signals. To measure the trigger efficiency, we use after-trigger-S2 signals from events taken in calibration runs. These S2 signals are recorded in data without trigger threshold effect. To achieve this, we set up another system with identical hardware as the new trigger system. Both systems use the same MAJ sum signal as the input. One system is used to generate the trigger for data taking, while another system, running the same trigger algorithm except that the requirement on trigger-wait time is relaxed, can still generate trigger output for these after-trigger-S2s during the same event. However, these trigger outputs do not affect the data taking and are only recorded by a V1724 digitizer for the efficiency measurement.

From the after-trigger-S2 signals and those satisfying the trigger condition (the spectrum is shown in Fig. 5 left), we derive the trigger efficiency of the new trigger system, shown in Fig. 5 right. A Fermi-Dirac ( $f(x) = 1/(e^{\frac{p_0-x}{p_1}} + 1)$ ) fit shows a 50% trigger efficiency is achieved for S2 around 50 PE, compared to 79 PE of the old trigger system [2]. Given that the single electron gain is approximately 25 PE/e [2], this corresponds to an average trigger threshold of about 2 single electrons.

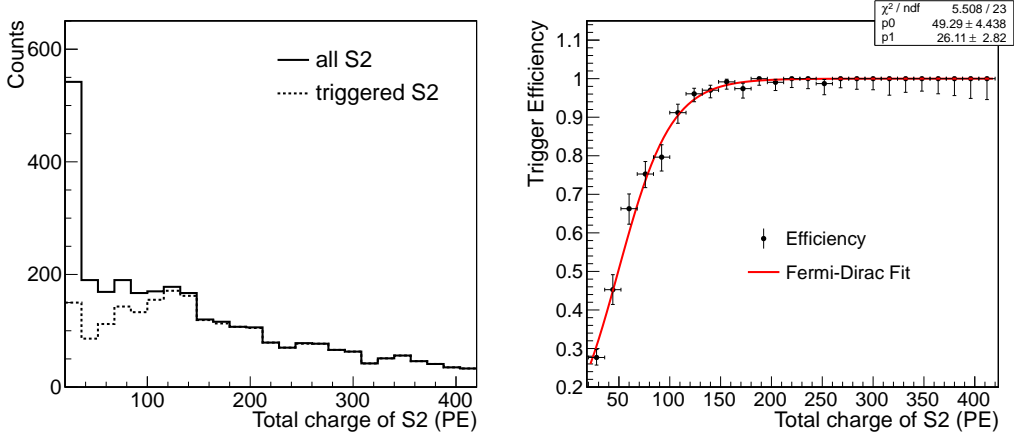


**Figure 5.** Left: Charge spectrum of all after-trigger-S2 and these satisfying the trigger condition. Right: trigger efficiency as a function of the S2 charge. A fitted Fermi-Dirac function is superimposed.

### 4 Summary

In conclusion, we presented a new trigger system developed for PandaX-II experiment. Compared to the previous analog-based trigger system, the new one uses a FPGA device to process digitized data and is significantly improved on flexibility and performance. The new system can effectively reduce mistriggering on afterpulses or discharge events. Besides, S2 signals can be triggered with a lower threshold. The new trigger system has been fully commissioned and deployed for data taking in PandaX-II.

## Acknowledgments

This project has been supported by a 985-III grant from Shanghai Jiao Tong University, grants from National Science Foundation of China (Nos. 11435008, 11455001, 11525522), a grant from the Ministry of Science and Technology of China (No. 2016YFA0400301) and a grant from the Office of Science and Technology in Shanghai Municipal Government (No. 11DZ2260700). Yong Yang is partially supported by a grant from Young 1000-plan program of China (No. GKKQ0720033). We thank Jun Hu and Xiaoshan Jiang at the Institute of High Energy Physics (IHEP) of the Chinese Academy of Sciences for useful discussions and help on the trigger algorithm.

## References

- [1] Andi Tan, Xiang Xiao, Xiangyi Cui, Xun Chen, Yunhua Chen, Deqing Fang, Changbo Fu, Karl Giboni, Franco Giuliani, Haowei Gong, et al. Dark matter search results from the commissioning run of PandaX-II. *Physical Review D*, 93(12):122009, 2016.
- [2] Andi Tan, Mengjiao Xiao, Xiangyi Cui, Xun Chen, Yunhua Chen, Deqing Fang, Changbo Fu, Karl Giboni, Franco Giuliani, Haowei Gong, et al. Dark matter results from first 98.7 days of data from the PandaX-II experiment. *Physical Review Letters*, 117(12):121303, 2016.
- [3] Changbo Fu, Xiangyi Cui, Xiaopeng Zhou, Xun Chen, Yunhua Chen, Deqing Fang, Karl Giboni, Franco Giuliani, Ke Han, Xingtao Huang, et al. Spin-Dependent WIMP-Nucleon Cross Section Limits from First Data of PandaX-II experiment. *Physical Review Letters*, 118(7):071301, 2017.
- [4] Mengjiao Xiao, Xiang Xiao, Li Zhao, Xiguang Cao, Xun Chen, Yunhua Chen, Xiangyi Cui, Deqing Fang, Changbo Fu, Karl Giboni, et al. First dark matter search results from the PandaX-I experiment. *Science China Physics, Mechanics & Astronomy*, 57(11):2024–2030, 2014.
- [5] CAEN V1724 manual. <http://www.caen.it/csite/>.
- [6] Xiangxiang Ren, Xun Chen, Xiangdong Ji, Shaoli Li, Siao Lei, Jianglai Liu, Meng Wang, Mengjiao Xiao, Pengwei Xie, and Binbin Yan. The electronics and data acquisition system for the PandaX-I dark matter experiment. *Journal of Instrumentation*, 11(04):T04002, 2016.
- [7] ANALOG DEVICES. <http://www.analog.com/en/index.html>.